

Observation of Particle Behavior in Fine Particle Peening process

Y. Aiba¹, K. Murai², M. Omiya² and J. Komotori²

¹ Graduate School of Science and Technology, Keio University, JAPAN

² Department of Mechanical Engineering, Keio University, JAPAN

Abstract

In this paper, we focused on the particle velocities of fine particle peening process (FPP) and measured them by a high-speed camera. Also, we developed the theoretical model of particle motions with the effect of jet flow and calculated the particle velocities after spouting from the nozzle. Then, we compared the experimental results with the calculated results, and those agreed well each other. It is concluded that the particle velocity can be estimated by our proposed model and it is helpful information for understanding the surface modification in fine particle peening (FPP) process.

Keywords: Fine particle peening (FPP), Particle velocity, jet flow

Introduction

Fine particle peening (FPP) process is one kind of surface modification process. FPP hardens treated materials and induces residual stresses, which enhances fatigue life. The efficiency of surface modification is influenced by many parameters such as material properties, particle size, particle amount, air pressure and so on. Especially, it is well known that particle velocity significantly influences the surface modification. However, since the particle sizes of FPPs are too small, the detail observation of particle behavior have not been studied.

In this study, to investigate the particle behavior in FPP process in detail, theoretical model of particle behaviors in FPP process was developed. Especially, we focused on the particle velocities during FPP and considered the effects of jet flow. Then, we calculated the particle velocities after spouting from the nozzle. Also, we measured particle velocities during FPP process by a high-speed camera. Then, we compared the calculated results with the experimental results.

Experimental Methods

1. Modeling of particle behavior

To make detail modeling about particle behavior, we at first focus on the jet flow from the nozzle. Turbulent jet forms three regions, those are schematically described in Figure 1 [1,2]. In its initial stage of development, the region near a nozzle exit and along the center of jet is called as potential core region. In this region, mean velocity is almost uniform.

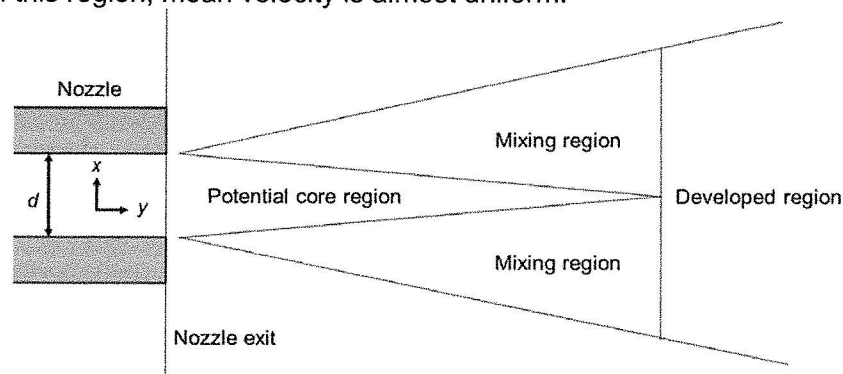


Figure 1 Turbulent jet flow from nozzle exit.

The region surrounding with the potential core region is called as mixing region. Over the distance from the nozzle, the jet becomes a fully developed and forms the developed region. The distance at the end of potential core region from the nozzle exit, y_c , can be described as $6d$, where d is the diameter of the nuzzle [1].

When particles are path through these regions, they are accelerated by the force from the jet. The equation of motion for particles may be described as,

$$m \frac{d^2 y}{dt^2} = \frac{\pi D^2}{8} C_D \rho_a(y) \{u(x, y) - v(x, y)\}^2, \quad (1)$$

where m is the particle mass and C_D is the coefficient of drag. For the spherical shape in turbulent flow, C_D is determined by the Reynolds number [3]. $\rho_a(y)$ is the air density. D is the particle diameter. $u(x, y)$ is the air velocity and $v(x, y)$ is the particle velocity. The term of velocity means the relative velocity between air and particles. Particles are assumed to accelerate along with y axis.

Air density, $\rho_a(y)$, and air velocity, $u(y)$, depends on the region where the particle is. Air density in atmosphere, ρ_{ab} , is assumed to be 1.205 kg/m^3 [4], air density in the compressor, ρ_{at} , as,

$$\rho_{at} = \rho_{ab} \frac{P + P_b}{P_b} = 1.205 \frac{P + P_b}{P_b}, \quad (2)$$

where P is the pressure of the compressor and P_b is atmospheric pressure [5]. We also obtain the air density in the nozzle, ρ_{as} , as,

$$\rho_{as} = 0.634 \rho_{at} = 0.764 \frac{P + P_b}{P_b}. \quad (3)$$

Air density in potential core region, $\rho_{ap}(y)$, is equal to air density at compressor, ρ_{as} , as [6],

$$\rho_{ap}(y) = \rho_{as}. \quad (4)$$

Air density in development region, $\rho_{ad}(y)$, can be described as [1,6],

$$\rho_{ad}(y) = \rho_{as} - (\rho_{as} - \rho_{ad}) \frac{y}{y - y_c}. \quad (5)$$

In this study, we define a_0 as the speed of sound and the flow is isentropic, air velocity at the nozzle exit, u_i , can be written as [4],

$$u_i = \frac{Q}{A}, \quad (6)$$

$$\frac{u_i^2}{2} = \frac{a_0^2}{\kappa - 1} \{1 - (P_e / P)^{(\kappa - 1)/\kappa}\}, \quad (7)$$

where Q is the flow rate measured at the nozzle of the experimental equipment. A is the cross sectional area at the nozzle. κ is specific-heat ratio of the compressive air, P is the pressure of compressor and P_e is the pressure at the nozzle exit [4].

In the potential core region, air velocity, $u(y)$, can be preserved. Thus, air velocity in the potential core region, $u_p(y)$, is [7],

$$u_p(y) = u_i. \quad (8)$$

The air velocity in the developed region, $u_d(y)$, can also be written as [7],

$$u_p(y) = u_i \frac{y_c}{y}. \quad (9)$$

Then, we calculate the theoretical value of the particle velocity solved numerically Eq. (1) by the Runge-Kutta method [8].

2. Measurement of particle velocities during FPP process

The particle behaviors during FPP process were measured with a high-speed camera. Target material was A5052 aluminum plate, which was $100 \text{ mm} \times 100 \text{ mm}$ in plane and the thickness was 10 mm . The shot particles used in this study are summarized in Table 1. The experimental apparatus is shown in Figure 2. The nozzle length, l_n , is 40 mm , and its diameter, d , is 6 mm . Projection distance from the nozzle exit to the specimen is 100 mm . Shot particles are supplied

from the inlet of the nozzle. The center of the specimen is just under the nozzle exit. Table 2 shows the experimental conditions.

The particle behavior during FPP process were observed with the high-speed camera (MEMRECAM-HX-1, nac Image Technology inc.) at three locations, those are 2 mm, 36 mm and 98 mm away from the nozzle exit. The particles velocities were analyzed by image analyses software (HXLink, nac Image Technology inc.).

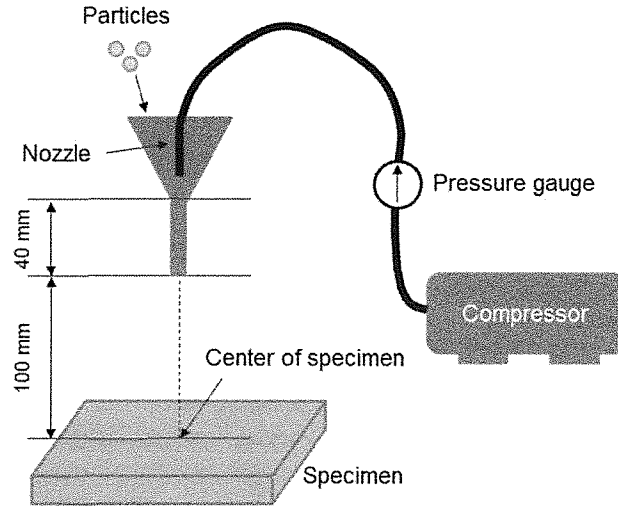


Figure 2 Experimental equipment of FPP.

Table 1 Particles used in FPP experiments.

Particle diameter D [microns – mm x 10^{-3}]	Material	Particle density [kg/m ³]
800, 400	High carbon-chromium	7800
200, 80	High-speed steel	7850
50	Chromium	7090

Table 2 Experimental conditions.

Experimental number	Particle diameter D [microns – mm x 10^{-3}]	Pressure P [MPa]
1	800	0.2
2	800	0.4
3	800	0.6
4	400	0.2
5	400	0.4
6	400	0.6
7	200	0.2
8	200	0.4
9	200	0.6
10	80	0.2
11	80	0.4
12	80	0.6
13	50	0.2
14	50	0.4
15	50	0.6

Experimental Results and Discussions

Figure 3 shows the comparison of the particle velocity between the theoretical and the experimental results. In these figures, the solid line is the theoretical value and the plot is the experimental value. Each figure corresponds to the particle diameter of 800μm, 400μm and 200μm. From these results, the theoretical results are consistent with the experimental results. The particles are accelerated by jet flows and the particle velocities become constant at almost 60 mm away from the nozzle exit.

Figure 4 shows the particles velocity at the location 2 mm away from the nozzle exit. Figure 5 also shows the particles velocity at the location 98 mm away from the nozzle exit. From these figures, as the particle size is smaller or the air pressure increases, the particle velocities increases.

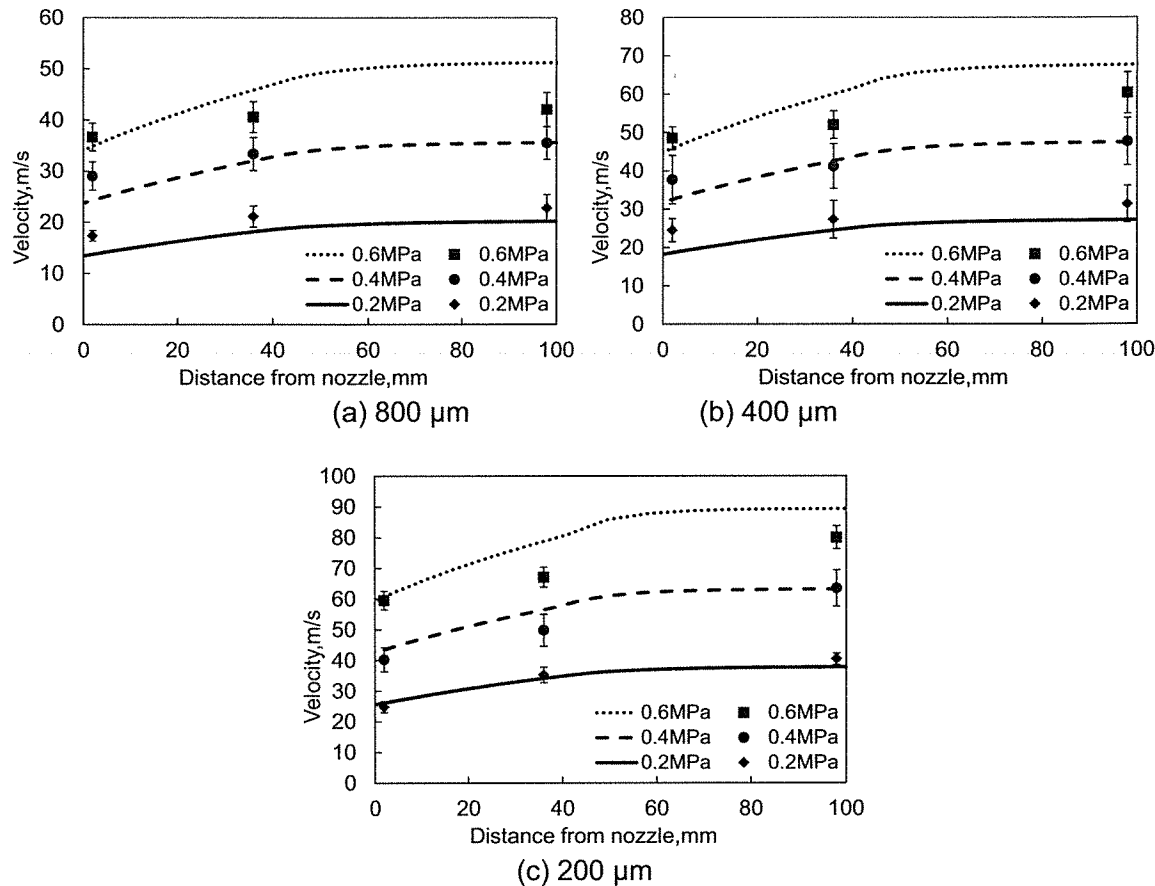


Figure 3 Particle velocities obtained by experiments and theoretical models.

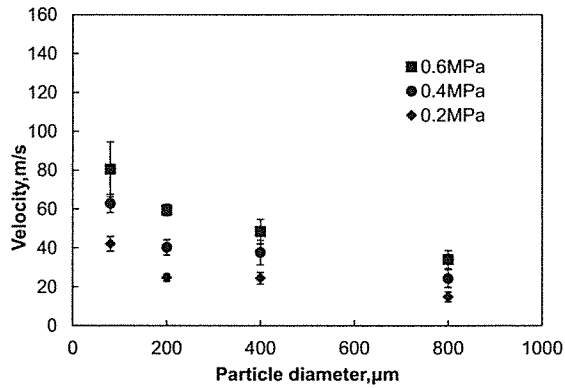


Figure 4 Particles velocity at 2 mm.

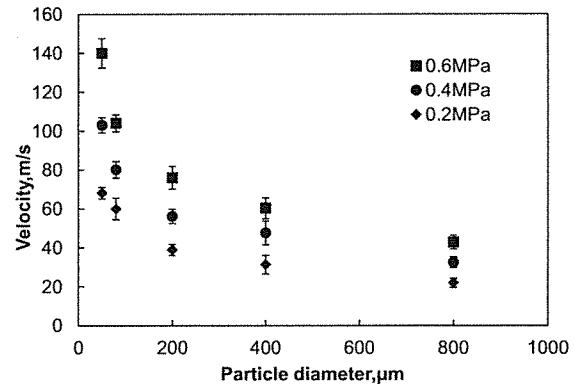


Figure 5 Particles velocity at 98 mm.

Summary

In this paper, to investigate the particle behavior in FPP process in detail, theoretical model of particle behaviors in FPP process was developed. Also, we measured particle velocities during FPP process by a high-speed camera. The obtained results showed that the particle velocities of the theoretical model are consistent with those of the experimental results. As the particle diameter decreases or the air pressure increases, the particle velocity increases. It is concluded that the particle velocity can be estimated by our proposed model and it is helpful information for understanding the surface modification in FPP process.

Acknowledgement

We gratefully acknowledgement nac Image Technology inc. for using high-speed camera. We express our gratitude to Mr. Someya for his kind help.

References

- [1] T. Shakouchi, *Jet Flow Engineering - Fundamentals and Application* -, Morikita, (2004).
- [2] H. Tennekes and J.L. Lumley, *A first course in turbulence*, Cambridge, MIT Press, (1972).
- [3] K. Watanabe and H. Kui, *Drag of a Sphere in High-Reynolds-Number Range in Water*, Transactions of the Japan Society of Mechanical Engineering, Vol. 62, No. 10 (1996), pp. 78-83.
- [4] F.M. White, *Fluid mechanics Sixth Edition*, McGraw-Hill, (2008).
- [5] K. Ogawa, T. Asano, A. Saito, K. Kawamura, M. Ogino and H. Aihara, *Measurement and Analysis of Shot Velocity in Pneumatic Shot Peening*, Transactions of the Japan Society of Mechanical Engineers, Vol. 60, No. 571(1994), pp. 1120-1125.
- [6] Y. Tomita, *Introduction to fluid mechanics*, Yokendo, (1971).
- [7] S. Harada and S. Ozaki, *Ryushi Engineering*, Yokendo, (1969)
- [8] K. Nanbu, K. Ito and N. Egami, *Numerical Calculation of Particles Velocity under the Compressible Fluid in Fine Particle Bombardments*, Transactions of the Japan Society of Mechanical Engineers, Vol. 76, No. 772 (2010), pp. 3728-3735.